INVESTIGATION OF THE PERFORMANCE OF SHORT DIFFUSER CONFIGURATIONS FOR DIFFERENT INFLOW PROFILES

J.Walter[1], D.Wurz[2] and M. Gabi[1]

[1]Karlsruhe Institute Of Technology, Institute of Fluid Machinery, Karlsruhe, Germany

[2]Emissionsmesstechnik und Strömungsmechanik (ESG), Baden-Baden, Germany

ABSTRACT

Diffusers are used to connect the outlet of axial fans to the following piping. In thermal power plants the diffuser design is often restricted by limited installation space. Two different diffuser configurations for limited diffuser length and fixed inlet and outlet diameter are studied at a scaled diffuser test rig. Configuration 1 combines an annular diffuser and a Carnot diffuser to achieve the required diffuser outlet diameter. Configuration 2 consists of an annular diffuser (diffuser 1) and a diffuser 2 with installed guiding bodies. These bodies are arranged in a star-like configuration and reduce the effective opening angle of the diffuser. The tests have been carried out with different inlet velocity profiles. Configuration 1 was more sensitive on inlet profile variation regarding flow separation. The pressure recovery for both configurations is compared for different positions downstream the diffuser. There is a significant static pressure increase due to a reduction of over-speed areas.

ANNULAR DIFFUSER, CARNOT DIFFUSER, WAKE AREA, PRESSURE RECOVERY, WALL SHEAR STRESS

NOMENCLATURE

B	blocked area fraction [-]
c_f	friction coefficient [-]
c_m	meridional velocity [m/s]
cp	coefficient of pressure recovery [-]
L	length [m]
p	pressure [Pa]
p_{dyn}	dynamic pressure [Pa]
p_{tot}	total pressure [Pa]
r	radial coordinate [m]
Re	Reynolds number [-]
s	position in annular gap [m]
S	annular gap height at diffuser inlet [m]
x	coordinate x axis [m]
α	opening angle of diffuser [°]
τ	wall shear stress [N/m²]
k	roughness [mm]

Sub/Superscripts

$\underline{hyd}$	hydraulic diameter
$\overline{( )}$	area average

Abbreviations

C1	Configuration 1
C2	Configuration 2
HOM	Undisturbed profile
T1	Tipstrong profile 1
T2	Tipstrong profile 2
MP	Measurement plane

INTRODUCTION

Axial fans are used in power plants for fresh air supply and flue gas transport. A typical configuration consists of an axial fan and an annular diffuser which connects the fan to the following piping (Figure 1). A large part of the total pressure increase of the fan is available as dynamic pressure at the fan outlet. In order to achieve a high efficiency of the configuration the dynamic pressure at the fan outlet needs to be converted in a static pressure increase. Therefore annular diffusers are used. In power plant application the diffuser design is often restricted by limited installation space and construction costs. Common configurations combine an annular diffuser and a Carnot diffuser to achieve the required diffuser outlet diameter for a restricted diffuser length. Downstream the annular diffuser a wake area is formed due to the abrupt end of the hub. The sudden diameter change at the housing causes a recirculation region. This leads to undesired flow instabilities which might cause further losses depending on the arrangement of the following components (e.g. silencer or elbow). Moreover, this can result in a damage of components due to vibrational excitation. Therefore it is desirable to achieve a stable forward flow downstream the housing of the annular diffuser.

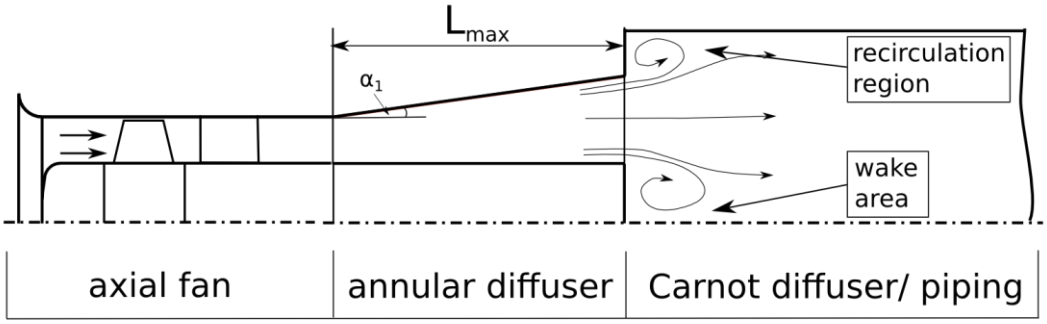

Figure 1: Schematic view of a typical fan-diffuser-piping configuration

There are various studies on annular diffuser design. The most notable work was published by Sovran and Klomp (1967). Their diffuser performance chart is widely used as a guideline for diffuser construction, giving a relation between length, area ratio and maximum pressure recovery. The influence of different hub geometries on the wake area downstream the hub is studied by Kalayeh et al (2015). They figured out that an ellipsoidal hub extension increases the pressure recovery. It is shown by various authors that the diffuser inlet profile has a strong effect of the diffuser performance (Zierer, 1995, Stevens and Williams, 1980, Japikse, 2002). Stevens and Williams showed that increased inlet turbulence can significantly increase the diffuser performance and the flow stability downstream. If the diffuser is arranged downstream a fan, the diffuser flow is strongly influenced by the fan outlet profile. The fan outflow is dependent on operation point and constructional characteristics. In power plant application diffusers operate usually at high Reynolds numbers ($Re_{hyd}>10^5$). The goal of this study is the investigation of two diffuser configurations at different diffuser inlet profiles for fixed diffuser length. Special attention is paid to the wall shear stress at the housing. Experiments were carried out on a scaled axial diffuser test rig. The impact of three different inlet velocity profiles is analyzed. Two inlet profiles are reproduced on the basis on in-situ measurements of power plant fans. Wall shear stress, total pressure and pressure are recorded at the test rig.

DEFINITIONS

Configuration 1 (C1) consists of an annular diffuser and a Carnot diffuser. The annular diffuser is constructed according to Sovran and Klomp (1967). The schematic view is shown in Figure 1.
Configuration 2 (C2) consists of an annular diffuser (diffuser 1) and a diffuser 2 with installed guiding bodies (Figure 2). They are arranged in a star-like configuration and reduce the effective opening angle of the diffuser. These bodies have a slender nose and an increasing thickness in flow

direction. The cross section of the bodies is wedge-shaped in radial direction (Figure 4) and in streamline direction they have the shape of an isosceles triangle. This shape is shown in Figure 3 as cylinder intersection at B-B (Figure 2).

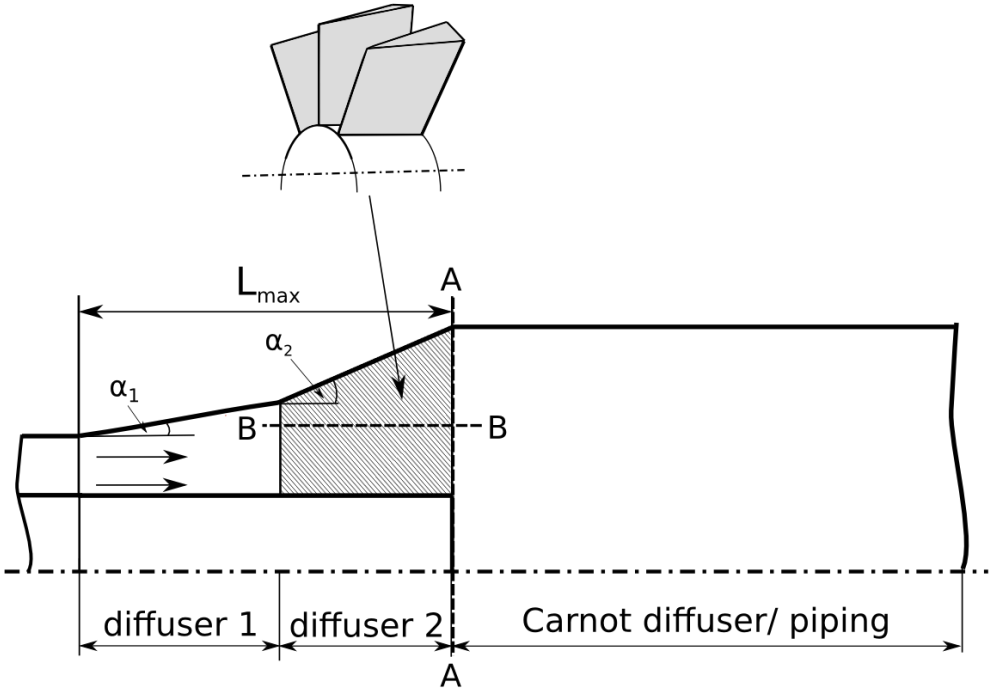

Figure 2: Schematic view of configuration 2 (C2)

The change of the cross-sectional area of diffuser 2 in streamwise direction is given in Figure 5. The area A at a position x/L_{Diff2} in diffuser 2 is related to the inlet area of diffuser 2 A(x/L=0). Diffuser inlet and outlet have equal cross sections. Up to around half of the diffuser 2 length the cross sectional area increases, while in the second half the effective flow area is reduced. This cross-sectional profile was chosen as a compromise between flow stability and manufacturing issues. The exit flow represents a multi-Carnot diffuser (Figure 4).

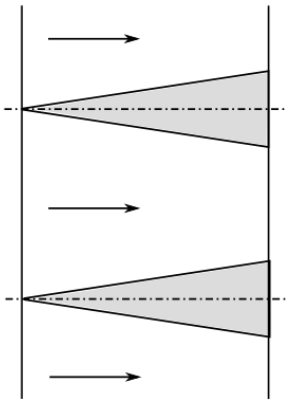

Figure 3: Developed Cylinder intersection at B-B

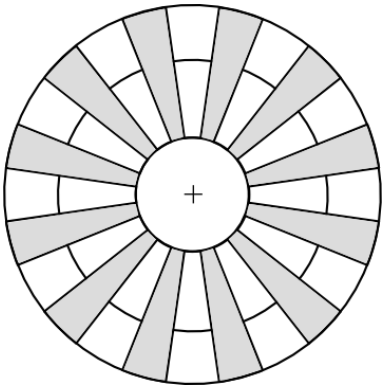

Figure 4: Schematic view at A-A, direction of view is upstream

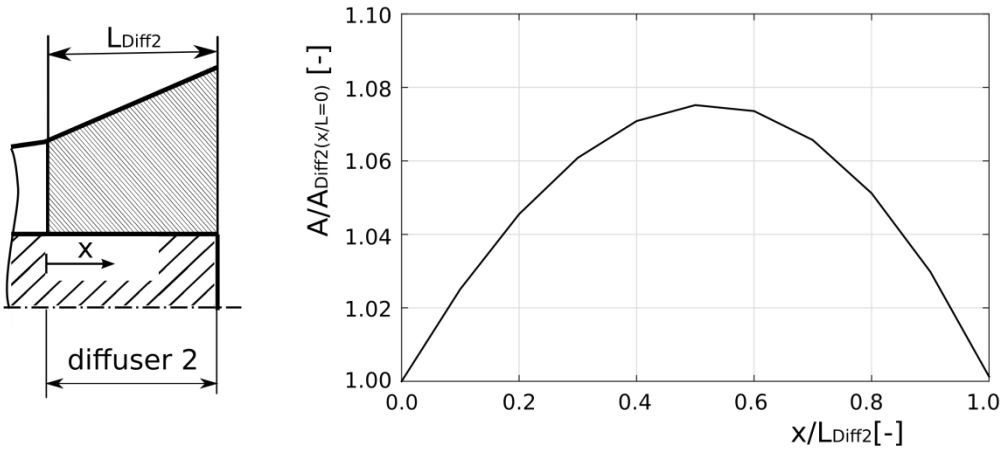

Figure 5: Streamwise variation of cross-sectional area $A/A_{Diff2(x/L=0)}$ in diffuser 2

Performance Parameters

Different parameters are introduced to describe the flow characteristics. The quantities which are area averaged are marked with a bar. The most important value is the pressure recovery coefficient. It is calculated by the static pressure increase and the dynamic pressure at the diffuser inlet:

$$c_{p,i} = \frac{\overline{p_i} - \overline{p_1}}{\overline{p_{dyn,1}}} \tag{1}$$

In order to quantify the blockage of the velocity profile at the inlet, the aerodynamic blockage is introduced analog to Sovran and Klomp (1967):

$$B = 1 - \frac{1}{A}\int \frac{c_m}{c_{m,max}} dA \tag{2}$$

EXPERIMENTAL SETUP

Test Rig

The test facility is shown in Figure 6. In order to obtain an air flow with low turbulence a plenum chamber with flow straightener and sieves is installed at the suction side of the test rig inlet. The rig is designed to conduct experiments at different inlet profiles, therefore an installation section for flow resistance sheets is arranged upstream the diffuser inlet. Downstream the annular diffuser is connected to a straight pipe. The installation is followed by a plenum chamber and centrifugal fan. There is a central axis to ensure the correct alignment of the hub in the center of the casing. The inlet section and the diffusers are made of sheet metal. The unfolded metal sheets and flanges are laser cut and satisfy a high manufacturing accuracy (+-0.05 mm). The cylindrical section downstream the diffuser is made of transparent material (Makrolon) for optical access. The roughness of both materials is smaller than k<0.06 mm (Wagner, 1992).

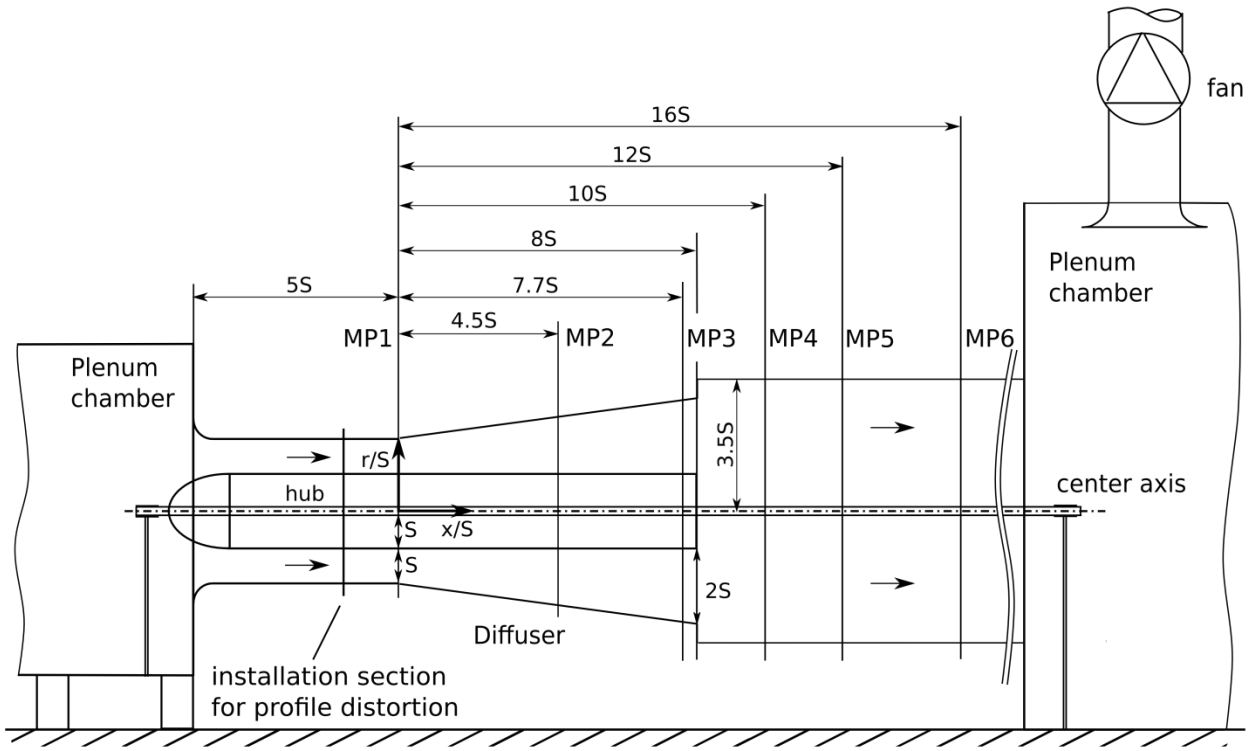

Figure 6: Test facility

Measurement Technique

Total and static pressure profiles are measured with pressure probes of different diameter. In the entry section and diffuser 1 a Prandtl probe with 3 mm diameter was used and for diffuser 2 and downstream a probe with 6 mm. The wall near measurements were conducted with a probe of 1mm diameter. The blocked area due to the insertion of the probe is for all measurement locations smaller than 0.01%. The temporal development of the pressure was monitored and the averaging was started when a stable mean value was achieved. For all measurements an integration time of at least 20s was chosen. The values were recorded with a pressure transducer with high accuracy (Range=0…500Pa, max. Error=0.07%) at a sample rate of 1000 Hz. The quality of the spatial averaged data is very dependent on the location of the measurement points in the duct section. In order validate these results a continuous volume flow measurement was installed. A calibrated volume flow measurement nozzle was arranged upstream the inlet of the centrifugal fan. The volume flow which was determined by the nozzle and the grid measurements at different measurement planes (MP) were compared. For all configurations a deviation of less than 1% was achieved at MP1. In the measurement planes downstream MP1, especially in planes with separated flow regions, the deviation was higher (max. 5%). The wall near velocity measurements were corrected with the displacement correction according to McMillan (Wuest, 1967). The static pressure at the wall of hub and housing was recorded. For the determination of the wall shear stress a Preston method (Preston, 1954) was used with the calibration curve of Patel (Pozzorini, 1976). There are various literatures on wall shear stress measurement according to Preston. Pozzorini (1976) did wall shear stress measurements in a conical diffuser with different methods and found a good agreement of the Preston method with the other methods. In this work the wall shear stress τ is related to the wall shear stress of a flat plate at equivalent outer flow velocity τ_{ref}. Under these considerations the ratio of the stresses equals the ratio of the friction coefficients ($\tau/\tau_{ref} = c_f/c_{f,ref}$). The reference friction coefficient $c_{f,ref}$ is calculated according to Schlichting (1979).

$$c_{f,ref} = (2\log_{10}(Re_x) - 0.65)^{-2.3} \quad (3)$$

Measurement sections

Profile measurements were conducted in the annular diffuser at the inlet (MP1, x/S=0), at x/S=4.5 (MP2) and close to the end of diffuser (MP3, x/S=7.7). Furthermore measurements were conducted downstream the annular diffuser in the cylindrical pipe (Carnot diffuser) at MP4 (x/S=12), MP5 (x/S=14) and MP6 (x/S=16). In all measurement planes (MP) measurements were taken in three axes (0°, 120°, 240°). The wall shear stress and static pressure at the wall is measured at various positions at the test rig.

Diffuser inlet profiles

In the present study different inlet profiles are analyzed. Two inlet profiles are reproduced on the basis on in-situ measurements downstream power plant fans. Measurements were taken at two configurations at nominal load downstream the impeller of the fan with Prandtl probes. The velocity profiles are averaged in circumferential direction (3 measurement axis). For both configurations the fan outlet profile is non-uniform. The velocity maximum is shifted to the outer region of the annular gap, while the flow near the hub lacks momentum. For Fan 1 (Figure 9) a maximum velocity of $c_{m,max}/\overline{c_m} = 1.16$ and for fan 2 (Figure 10) a $c_{m,max}/\overline{c_m} = 1.23$ was recorded. In order to reproduce these characteristic profiles, flow resistance sheets were designed (Figure 7). The schematic layout of these sheets is based on studies of Hirschmann (2012). The open area fractions of the sheets were adjusted to reproduce the profiles by means of CFD. The computational domain includes the inlet section, the flow resistant sheets and a cylindrical pipe section downstream the sheets. Due to rotational symmetry only a circular segment of the configuration was modelled (Figure 8). The steady RANS calculations were performed with the commercial CFD solver FLUENT. The open area fraction of flow resistance sheet T2 is in the hub near region smaller than the open area fraction of T1.

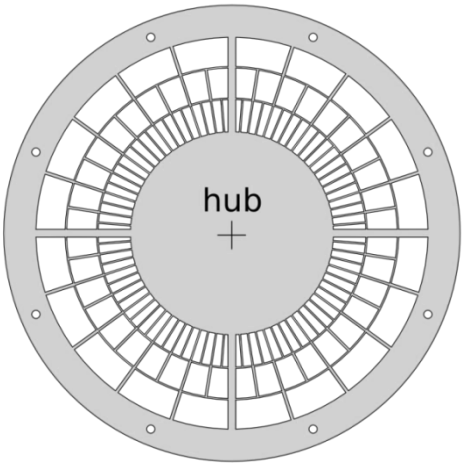

Figure 7: Flow resistance sheet

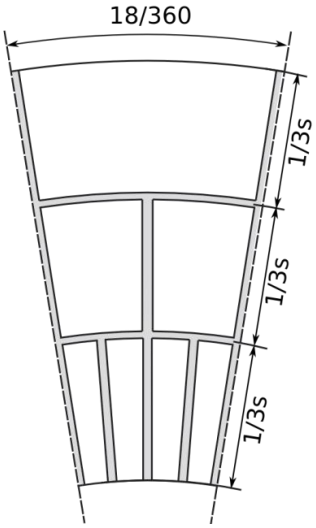

Figure 8: Circular segment for CFD

The velocity profiles which are determined by CFD are compared to the profiles in the test rig and the power plant (Fig. 9 and Fig. 10). The reconstructed profiles in the test rig reproduce the profiles which were measured in the power plant. The CFD results are in good agreement with the profiles in the test rig, only the middle and outer area of the annular gap for T1 is slightly over- respectively underrated. The velocity peak for configuration T1 (Figure 9) is slightly lower than in the power plant profile ($c_{m,max,power\ plant}/\overline{c_{m,power\ plant}}$ = 1.16, $c_{m,max,test\ rig}/\overline{c_{m,test\ rig}}$ = 1.12). The measurements were also conducted for an undisturbed inlet profile (Figure 11). The aerodynamic blockage of the inlet profiles is calculated. The blockage of uniform inlet profile is *B*=0. The inlet

profile characteristics are described in Table 1. For all tests a Reynolds independency can be expected ($Re_{hyd} > 10^5$, Traupel, 2003).

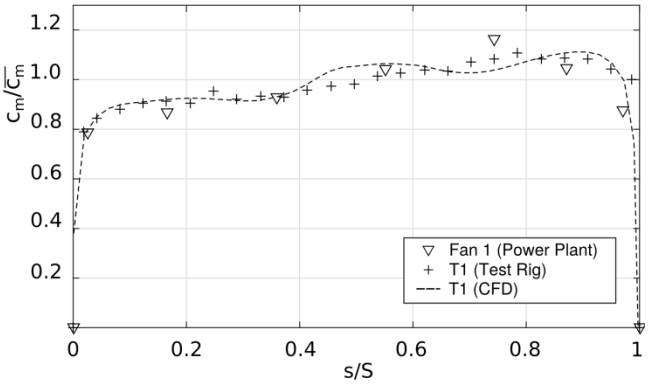

Figure 9: Reconstruction of profile T1

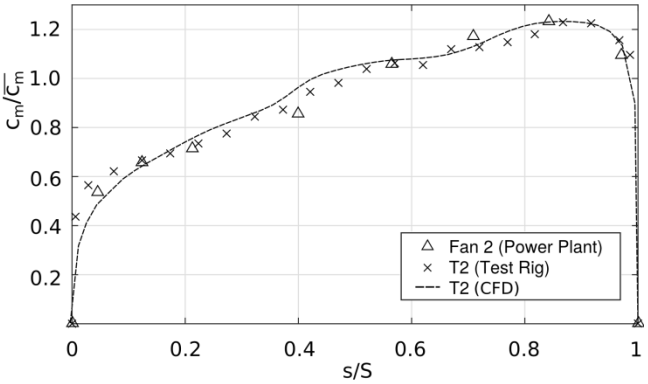

Figure 10: Reconstruction of profile T2

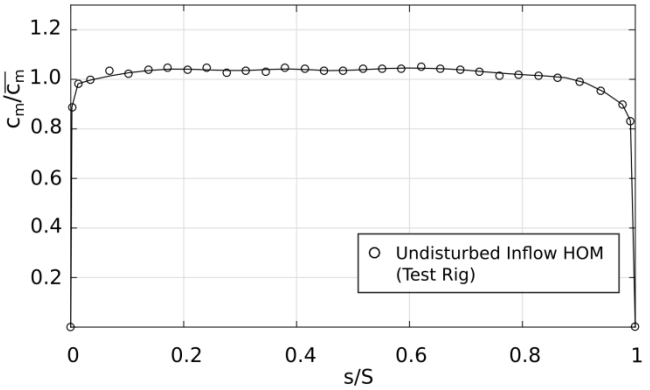

Figure 11: Undisturbed inflow profile HOM

Table 1: Characteristics of the inlet profiles

Inlet profile	$c_{m,max}/\overline{c_m}$	Re_{hyd} [-]	B [-]
T1	1.12	$3 \cdot 10^5$	0.099
T2	1.23	$3 \cdot 10^5$	0.186
HOM	1.04	$3 \cdot 10^5$	0.034

RESULTS AND DISCUSSION

Velocity Profiles

The velocity profiles of the annular diffuser and downstream are analyzed in the following section. First the profile development is shown for the undisturbed inlet profile (HOM). As can be seen in Figure 12 a velocity peak develops in the annular diffuser close to the hub. At the outlet of the annular diffuser no stable forward flow was measured at the housing. At x/S=12 the profile history is clearly visible, there is little volume flow close to housing and in the wake of the hub. For C2 (Figure 13) the influence of the guiding bodies in diffuser 2 is clearly present. The velocity profile is largely rehomogenized in the diffuser 2, leading to stable forward flow at hub and housing. Downstream diffuser 2 the velocity peak is shifted to the housing at x/S=12, while the wake area of the hub is extended. At x/S=16 the profiles in both configurations reach a similar level of homogeneity.

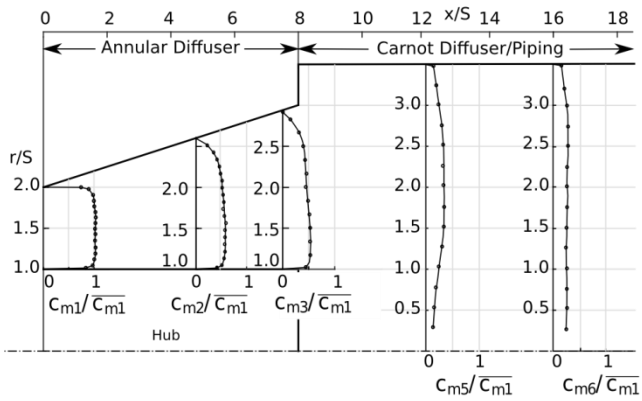

Figure 12: Flow profiles in C1 (left) for the undisturbed inlet (HOM)

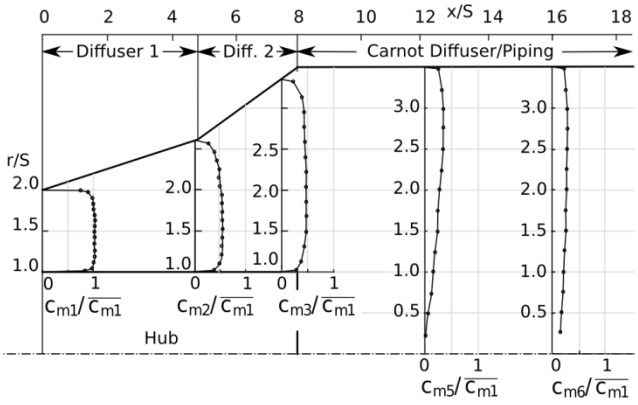

Figure 13: Flow profiles in C2 for the undisturbed inlet (HOM)

As mentioned in the introduction, the outflow of fans and blowers is not uniform but shows a distinct characteristic. The influence of the reconstructed tipstrong inlet profile 1 (T1) in C1 can be seen in Figure 14. The slight shift of the velocity peak to the outer area is enough to prevent separation in the annular diffuser at hub and housing. This leads to a more homogeneous profile at x/S=12 and x/S=16, especially the wake area at the casing is reduced. In C2 (Figure 15) the impact of the changed inlet profile (T1) is small. The profile gets rehomogenized in diffuser 2 and thus the outflow shows the similar characteristic downstream the diffuser 2 as for the undisturbed inflow (Figure 13).

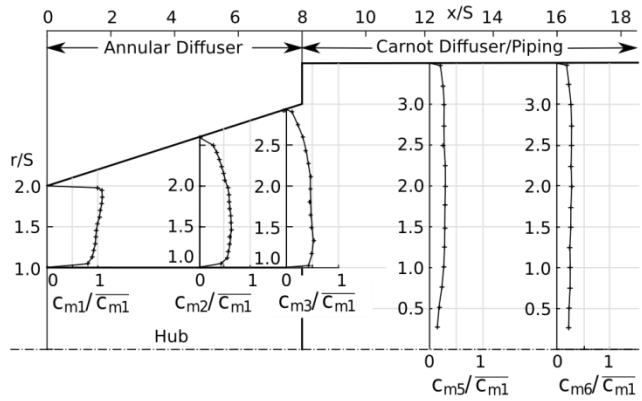

Figure 14: Flow profiles in C1 for inlet profile T1

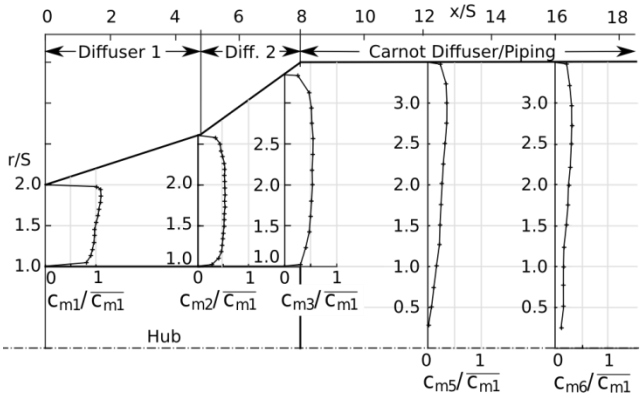

Figure 15: Flow profiles in C2 for inlet profile T1

The distorted inlet profile Tipstrong 2 (T2) is characterized by a high velocity peak close to the housing, while the hub lacks momentum. This leads in C1 (Figure 16) to flow separation at the hub in at x/S=4.5 and x/S=7.7, while there is a stable forward flow at the casing measured. In C2 (Figure 17) no separation can be detected in diffuser 1 and diffuser 2. However there is an extended wake area downstream the hub while the flow velocity in the outer region is increased.
Hirschmann et al. (2012) studied the influence of the total pressure profile in annular gas turbine diffusers. They generated a hubstrong, a uniform and a tipstrong inlet profile. Their findings for the flow field in the diffuser are in good agreement with the results in the annular diffuser of C1. The uniform profile tends to separate at the housing of the diffuser outlet, while the tipstrong separates at the hub.

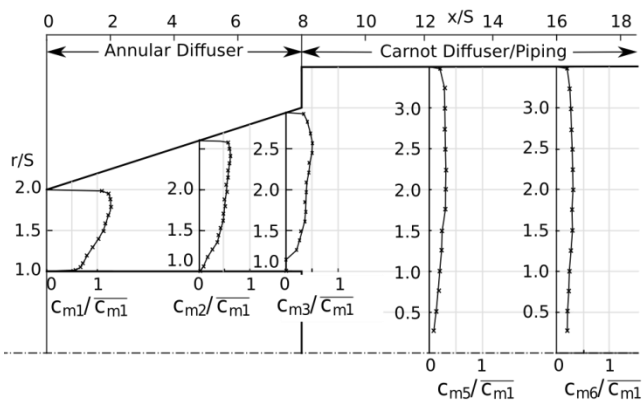

Figure 16: Flow profiles in C1 for inlet profile T2

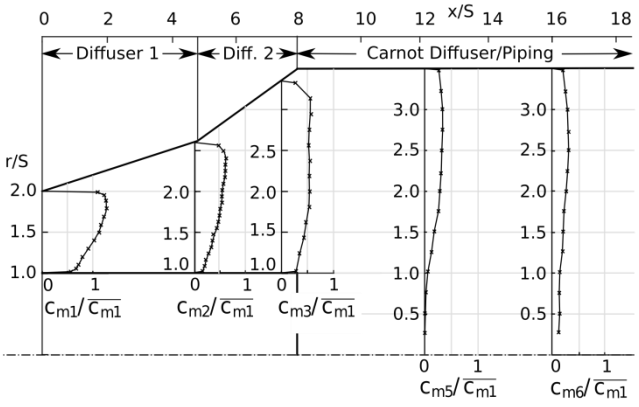

Figure 17: Flow profiles in C2 for inlet profile T2

Of great interest is the length of the wake areas downstream the guiding bodies in diffuser 2 of C2, respectively the length of the recirculation area downstream the Carnot diffuser at the housing of C1. Each body in C2 causes a separate wake area, while in C1 one recirculation area at the housing is formed. Since the axial length of the wake areas in C2 are dependent on the radial position, a reference position is defined. The reference position was chosen at $r_{ref} = 1/\sqrt{2} \cdot r_o \approx 2.5S$ (radius where half of the cross sectional area is reached). The velocity is measured in this region and related to the mean velocity. In order to find the point of reattachment in C1 the wall shear stress at the casing downstream the annular diffuser is determined. The results are shown in Figure 18 and Figure 19.

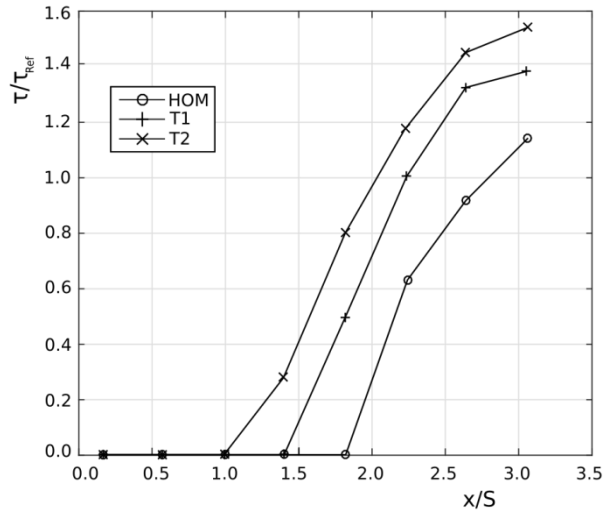

Figure 18: Wall shear stress downstream the annular diffuser of C1

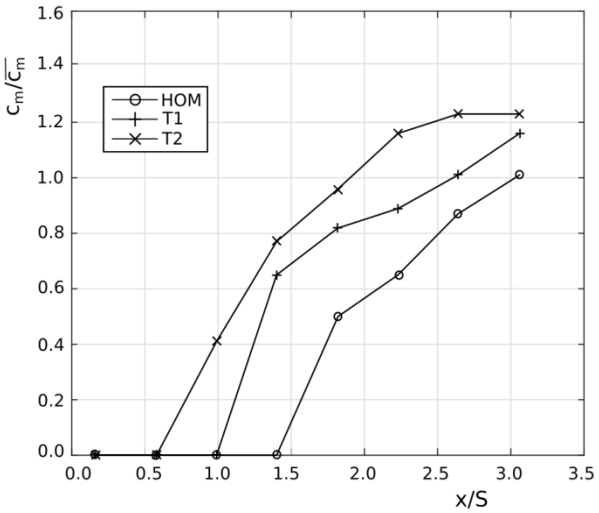

Figure 19: Meridional velocity c_m downstream diffuser 2 of C2 behind the wake area of the guiding bodies

The initial position where forward flow is measured is shown in Table 2 below. As can be seen the axial length of the wake area in C2 is smaller than in C1. For all inlet profiles a reduction of the wake area of approx. 0.4S is measured. Further downstream the mean velocities respectively the wall shear stresses are higher than reference values, this is due to the velocity peak close to the housing.

Table 2: Length of wake area for different inlet profiles

Configuration	C1	C2
Inlet Profile	x/S [-]	x/S [-]
HOM	2.2	1.8
T1	1.8	1.4
T2	1.4	1.0

Wall Shear Stress

A stable forward flow at the housing and the hub is necessary to achieve a symmetric flow to the following components downstream. A stable forward flow is of special interest in the diffuser, since perturbations in the flow are amplified due to the back pressure gradient. This is analytically shown by Banks et. al. (1987) for Jeffrey-Hamel flows. Positive wall shear stress indicates forward flow, while negative wall shear stress indicates flow separation. The probe alignment allows only a precise measurement of positive wall shear stress. Locations with negative values were set zero. First C1 is discussed (Figure 20). For the undisturbed inflow (HOM) the shear stress is higher at the hub than at the housing. Flow separation is detected at the housing of the annular diffuser at x/S>6. The profile T1 shows a forward flow at all measurement locations. The momentum deficit of Profile T2 close the hub leads to flow separation at x/S>4, while a stable forward flow is detected at the housing with high wall shear stress ($\tau/\tau_{ref} > 1$). This leads to a shortened recirculation area at the housing (Table 2) and an increased wake area downstream the hub. The diffuser 2 of C2 leads to a signifacant recovery of the wall shear stress (Figure 21). For all inlet profiles positive wall shear stress is measured in diffuser 2. Altough inlet profile T2 tends to spearate at the hub in diffuser 1, the flow reattaches in diffuser 2 due to the reduced opening angle in diffuser 2. Downstream diffuser 2 there is high wall shear stress recorded at the housing which is reduced downstream. Unlike C1, in C2 there is no recirculation area around the entire perimeter at the housing, the flow follows the contour of the casing downstream the flow section of diffuser 2.

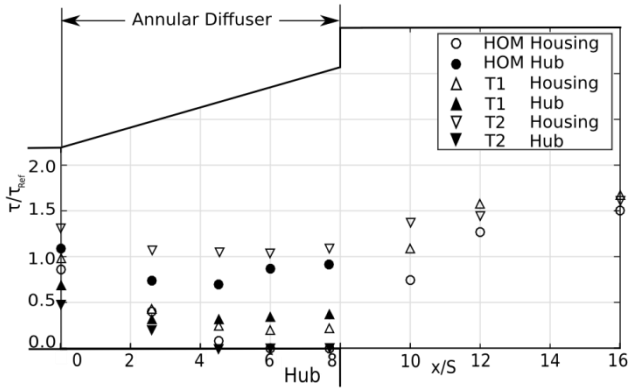

Figure 20: Wall shear stress of C1

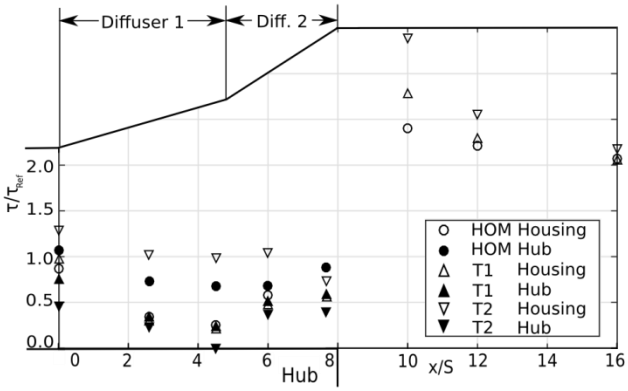

Figure 21: Wall shear stress of C2

Pressure Recovery

The pressure recovery coefficients *cp* for the different configurations and inlet profiles are analyzed. First the configuration C1 is discussed (Table 3). There is a significant variation of the pressure recovery especially in the measurement section close to the outlet of the annular diffuser (x/S=10). The profile T2 shows the lowest pressure increase at this position which is due to the large proportion of dynamic pressure. Further downstream (x/S>12) the pressure recovery is largely completed due to the wide rehomogenisation of the flow profiles.

Table 3: Pressure recovery cp of C1

x/S	HOM	T1	T2
10	0.71	0.73	0.66
12	0.73	0.74	0.71
16	0.74	0.74	0.73

In C2 the pressure recovery is less sensitive regarding the inlet profile (Table 4). At x/S=10 T2 gives a pressure recovery of cp=0.64 while the profile HOM leads to cp=0.68. The pressure recovery for all profiles start at a lower level compared to C1 and need therefore an increased length downstream for pressure recovery.

Table 4: Pressure recovery cp of C2

x/S	HOM	T1	T2
10	0.66	0.68	0.64
12	0.69	0.70	0.67
16	0.72	0.73	0.72

CONCLUSION

The approach to split the abrupt cross sectional change of C1 in several small parts leads to a stable forward flow at the casing for all investigated inlet profiles. The wall shear stress downstream the hub is higher for C2 compared to C1. Regarding flow stability this is advantageous, since the instabilities can cause further losses and damage. However the wake area of the hub is extended compared to configuration C1 and the flow needs more length for pressure recovery in C2. These results show that this approach seems promising but there is potential for optimization. On the one hand the effective opening angle of the diffuser 2 could be varied and on the other hand the wake area of the hub should be reduced. Therefore a variation of the hub geometry should be tested. Furthermore it is planned use these guiding bodies as a splitter silencer and investigate the acoustic properties.

ACKNOWLEDGEMENTS

This work is supported by the German Federal Ministry of Economics (BMWi) in scope of a ZIM project.

REFERENCES

Klomp, E., Sovran, G., 1967, *Experimentally determined optimum geometries for rectilinear diffusers with rectangular, conical or annular cross-section*, Fluid Mechanics Of Internal Flow, Proceedings of a symposium 20(21)

Rasouli Ghazi Kalayeh, K., Schäfer, P., Finzel, C., and Hofmann, W., 2015, *Experimental And Numerical Study Of A Gas Turbine Exhaust Diffuser Applying Different Hub Extension Geometries*, 11th European Turbomachinery Conference

Zierer, T, 1993, *Experimental investigation of the flow in diffusers behind an axial flow compressor*, ASME International Gas Turbine and Aeroengine Congress and Exposition

Stevens, S. J., Williams, G. J., 1980, *The influence of inlet conditions on the performance of annular diffusers*, Journal of Fluids Engineering, Vol. 102(3), pp. 357-363.

Japikse, D., 2002, *Correlation of annular diffuser performance with geometry, swirl, and blockage,* Proceedings of the 11th NASA/OSU Thermal and Fluids Analysis Workshop

Wuest, W., 1969, *Strömungsmeßtechnik: Lehrbuch für Aerodynamiker, Strömungsmaschinenbauer Lüftungs-und Verfahrenstechniker ab 5. Semester*, Springer-Verlag, pp.61

Wagner, Walter., 1992, *Strömung und Druckverlust: mit Beispielsammlung*, Vogel, p.79

Pozzorini, R.,1976, *Das turbulente Strömungsfeld in einem langen Kreiskegel-Diffusor,* Doctoral dissertation, ETH Zürich, Nr. 5646

Schlichting, H., 1979, *Boundary-layer theory,* Springer-Verlag

Preston, J., 1954, *The determination of turbulent skin friction by means of Pitot tubes*. Journal of the Royal Aeronautical Society, 58(518), 109-121.

Hirschmann, A., Volkmer, S., Schatz, M., Finzel, C., Casey, M., & Montgomery, M. ,2012, *The influence of the total pressure profile on the performance of axial gas turbine diffusers*, Journal of Turbomachinery, 134(2), 021017

Banks, W. H. H., Drazin, P. G., & Zaturska, M. B., 1988, *On perturbations of Jeffery-Hamel flow*, Journal of Fluid Mechanics, *186*, pp. 559-581.